Metabolic imaging via fluorescence lifetime imaging microscopy for egg and embryo assessment

Tim Sanchez, Ph.D.,[a] Man Zhang, M.D., Ph.D.,[b] Dan Needleman, Ph.D.,[a] and Emre Seli, M.D.[b]

[a] Department of Molecular and Cellular Biology and Faculty of Arts and Sciences Center for Systems Biology and John A. Paulson School of Engineering and Applied Sciences, Harvard University, Cambridge, Massachusetts; and [b] Department of Obstetrics, Gynecology and Reproductive Science, Yale University, New Haven, Connecticut

Current strategies for embryo assessment in the assisted reproductive technology laboratories rely primarily on morphologic parameters that have limited accuracy for determining embryo viability. Even with the addition of invasive diagnostic interventions such as preimplantation genetic testing for aneuploidy alone or in combination with mitochondrial DNA copy number assessment, at least one third of embryos fail to implant. Therefore, at a time when the clinical benefits of single ET are widely accepted, improving viability assessment of embryos is ever more important. Building on the previous work demonstrating the importance of metabolic state in oocytes and embryos, metabolic imaging via fluorescence lifetime imaging microscopy offers new and potentially useful diagnostic method by detecting natural fluorescence of FAD and NADH, the two electron transporters that play a central role in oxidative phosphorylation. Recent studies demonstrate that fluorescence lifetime imaging microscopy can detect oocyte and embryo metabolic function and dysfunction in a multitude of experimental models and provide encouraging evidence for use in scientific investigation and possibly for clinical application. (Fertil Steril® 2019;111:212–8. ©2018 by American Society for Reproductive Medicine.)

Key Words: Metabolism, mitochondria, embryo assessment, viability, non-invasive, NADH, FAD

Soon after the application of IVF into clinical practice (1), embryo quality was understood to be pivotal to treatment outcome (2). As such, it quickly became a central objective in assisted reproductive technologies to identify methods of accurately assessing embryo quality (3). An association between embryo morphology and cleavage rate and IVF outcome has been observed (4), and sophisticated morphological algorithms to identify embryos that are more likely to implant have been developed (5–8). However, the diagnostic accuracy of these approaches remained limited. More recently, time-lapse imaging has attempted to capture dynamic information regarding cleavage rate and morphology, in the hopes that this would be a strong predictor of viability; however, clinical trials have not demonstrated strong improvements in success rates (9–11).

In the absence of reliable assessment methods, clinicians resort to transferring multiple embryos to achieve higher success rates. However, as the risks associated with multiple pregnancies become increasingly more evident (12), practitioners have begun to prioritize achieving a healthy singleton birth at term (9, 13), which can be best accomplished by single ET (14). A single ET strategy further increases the importance of precise preimplantation embryo assessment and selection tools.

Embryo quality is determined by several factors. Chromosome copy number in embryonic cells is extremely important, as aneuploidy is highly associated with embryo failure (15–17). Preimplantation genetic testing for aneuploidy has demonstrated some improvement in IVF success (18–20). However, concerns exist regarding the consistency of these diagnostic methods (21) and around the impact of mosaicism on diagnostic accuracy (22, 23). In addition, preimplantation genetic testing for aneuploidy does not provide information about

Received December 3, 2018; accepted December 14, 2018.

T.S. is cofounder and a shareholder and officer of LuminOva and coholds patent US20150346100A1 pending for metabolic imaging methods for assessment of oocytes and embryos and patent US20170039415A1 issued for nonlinear imaging systems and methods for assisted reproductive technologies. M.Z. has no conflict of interest. D.N. is cofounder and a shareholder and officer of LuminOva and coholds patent US20150346100A1 pending for metabolic imaging methods for assessment of oocytes and embryos and patent US20170039415A1 issued for nonlinear imaging systems and methods for assisted reproductive technologies. E.S. is a consultant for and receives research funding from the Foundation for Embryonic Competence. E.S. has no conflict of interest regarding commercial application of fluorescence lifetime imaging microscopy technology.

Reprint requests: Emre Seli, M.D., 310 Cedar Street, LSOG 304B, New Haven, Connecticut 06520-8063 (E-mail: emre.seli@yale.edu).

Fertility and Sterility® Vol. 111, No. 2, February 2019 0015-0282/$36.00

https://doi.org/10.1016/j.fertnstert.2018.12.014

metabolic or other nongenetic viability parameters. The mitochondrial DNA (mtDNA) copy number (24) has been assessed as a proxy for the state of mitochondria, but results have not consistently shown a strong signal for predicting viability (25). Today, at least 35%–40% of euploid embryos still fail to implant (18). Therefore, the need for additional approaches that may help improve implantation rates remains. As there are a number of potential risks associated with invasive methods, the demand for noninvasive assessment strategies is especially high (26).

Embryo metabolic integrity is central to viability, and methods exist for assessing metabolism noninvasively. Attempts were made to measure glucose and pyruvate uptake by analyzing spent embryo media with microfluorometry (27). Gardner and Leese found that viable embryos had a significantly higher rate of glucose consumption than nonviable ones (28), again highlighting the importance of metabolism. Additionally, spent embryo culture media amino acid concentration has been associated with IVF outcome (29). However, efforts to translate this into a clinical tool failed due to technical complexities and the need for highly specialized equipment (13). Similarly, metabolomic assessments performing spectroscopic analysis on spent media have been attempted with some initial success in proof-of-concept studies (30, 31); however, subsequent randomized controlled trials failed to show a benefit (32, 33).

Metabolic imaging via fluorescence lifetime imaging microscopy (FLIM) is a new, noninvasive approach to measuring the biochemical status of embryos. It is a fluorescence technique (34) focusing on NADH and FAD. Because these molecules are naturally fluorescent and integral to cellular respiration (35), they provide a means of directly probing cellular mitochondrial metabolic status. This technique has been previously validated for distinguishing metabolic states in other biological systems, such as cancer cells (36), cell lines (37), animal tissues (38), and during germ cell differentiation in *Caenorhabditis elegans* and stem cells differentiation (39). Preliminary animal studies on oocytes and embryos indicate sensitivity to metabolic differences that are relevant in fertility. Recently, Sanchez et al. (40) showed that FLIM measurements were able to sensitively distinguish between metabolic states that are known to be different: [1] old versus young mice (40) and [2] oocytes from wildtype and knockout mice for the gene, *Clpp*, a mutation affecting metabolic function and fertility (41, 42).

FIGURE 1

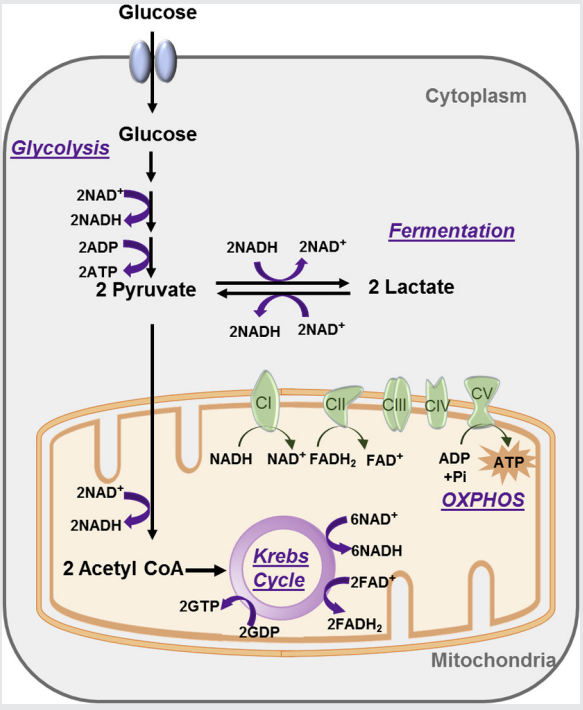

The role of mitochondria in cellular metabolism. Glycolysis occurs in the cytoplasm and converts glucose into two molecules of pyruvate. During glycolysis, two net molecules of ATP are gained and two molecules of NAD^+ are converted to NADH. Pyruvate molecules produced during glycolysis can be transported into the mitochondrial matrix and oxidized into AcCoA. A NADH is formed for each pyruvate molecule converted to AcCoA. In addition, for each acetyl group that enters the Krebs cycle, three molecules of NADH, one $FADH_2$, and one GTP are produced. The process of OXPHOS is mediated by the ETC located in the inner mitochondrial membrane and involves five protein complexes. ETC oxidizes NADH to NAD^+, $FADH_2$ to FAD, generating three and two ATPs per molecule, respectively. Therefore, glycolysis (anaerobic) generates two net ATP molecules per glucose, and in the presence of oxygen and a functional mitochondrial ETC, a total of 38 ATP molecules (including the two ATP generated during glycolysis) can be produced per glucose. In lactate fermentation, the pyruvate generated during glycolysis undergoes a redox reaction catalyzed by lactate dehydrogenase, forming lactic acid. In this process, two NADH molecules are converted (oxidized) to two NAD^+. Complex I (NADH-coenzyme Q oxidoreductase); complex II (succinate-Q oxidoreductase); complex III (Q-cytochrome c oxidoreductase); complex IV (cytochrome c oxidase); complex V (ATP synthase).

Sanchez. FLIM for egg and embryo assessment. Fertil Steril 2018.

THE ROLE OF MITOCHONDRIA IN CELLULAR METABOLISM

Glycolysis (Fig. 1) is the metabolic pathway that converts glucose (a 6-carbon molecule [6C]) into two molecules of pyruvate (3-carbon molecule; [3C]). Glycolysis takes place in the cytoplasm and does not require oxygen. The free energy released in this process is used to gain two net molecules of ATP and to convert two molecules of NAD^+ to NADH.

Pyruvate molecules produced during glycolysis can be transported into the mitochondrial matrix and oxidized into acetyl CoA (AcCoA), leading to the formation of NADH (one for each pyruvate molecule converted to AcCoA) and facilitating the start of the Krebs cycle for additional energy production. For each acetyl group that enters the Krebs cycle, three additional molecules of NADH, one $FADH_2$, and one GTP are produced. The NADH and $FADH_2$ molecules can then be used to create additional ATP through oxidative phosphorylation (OXPHOS) (43).

The process of OXPHOS is mediated by the electron transport chain (ETC) located in the inner mitochondrial membrane and involves five protein complexes (Fig. 1). NADH and $FADH_2$, are oxidized by complex I (NADH-coenzyme Q oxidoreductase) and complex II (succinate-Q

oxidoreductase) of the ETC, respectively. The added electrons at complexes I and II are then relayed along the ETC and help generate a proton gradient between the mitochondrial intermembranous space (higher) and the mitochondrial matrix (lower). Finally, the movement of protons through the ATP synthase (complex V), along the proton gradient (from the mitochondrial intermembranous space to the mitochondrial matrix), results in the generation of ATP. Overall, the ETC oxidizes NADH to NAD^+, and $FADH_2$ to FAD, generating three and two ATPs per molecule, respectively (44). While glycolysis generates only a net total of two ATP molecules per glucose molecule, the Krebs cycle and ETC result in the synthesis of an additional 36 ATPs for each glucose metabolized (Fig. 1).

NAD^+ and FAD play a vital role in energy metabolism in eukaryotic cells by accepting hydride equivalents to form reduced NADH and $FADH_2$. These furnish reducing equivalents to the mitochondrial ETC to fuel OXPHOS. NADH is a product of both the glycolysis (in the cytoplasm) and the Krebs cycle (in the mitochondrial matrix), while $FADH_2$ is only produced in the Krebs cycle (Fig. 1). Since the mitochondrial membrane is not permeable to NAD^+ (45), the reduced form of NADH generated in the cytoplasm can be transported into the mitochondrial matrix via either the malate-aspartate shuttle or the glycerol-3-phosphate shuttle of the inner mitochondrial membrane (46). Importantly, even in the presence of an excess of glucose, inadequate NAD^+ could block glycolysis and NADH production, leading to cell death (47, 48).

When insufficient oxygen is available to support OXPHOS, pyruvate generated from glycolysis can be converted into lactate by lactate dehydrogenase through a process called lactate fermentation (Fig. 1). Fermentation allows the recycling of NADH back into NAD^+ so that glycolysis can continue. This process does not require oxygen and occurs in muscle when the need for energy surpasses what OXPHOS can produce.

FLIM MICROSCOPY

NADH and FAD are fluorescent molecules, which means that shining light on them of one wavelength can cause them to transition to an excited state and emit light of another wavelength as they relax back to their ground state (34). Fluorescence microscopy takes advantage of this property to specifically visualize fluorescent molecules by selectively controlling the wavelength of the exciting light and using optical filters to only view light emitted by the molecule of interest (Fig. 2A). NADH and FAD have absorption and emission spectra that are highly distinct from each other (Fig. 2B), and from other cellular components (49), making it possible to study the behavior of these two molecules in vivo. Since the pioneering work of Chance and collaborators nearly 60 years ago (50), fluorescence microscopy of NADH and FAD has been widely used to characterize the metabolic state of mitochondria, cells, and tissues (38, 51–53).

Fluorescence microscopy of NADH and FAD provides morphological information, including allowing the visualization of mitochondria, in which both molecules are highly enriched. The measured fluorescence intensity also reflects the activity of the pathways that these molecules are engaged in because the brightness of the fluorescence signal from these molecules is proportional to their concentration. While such intensity measurements are highly informative, they suffer from two major limitations: [1] the concentration of NADH and FAD reflects the relative balance of biochemical pathways, so very different physiological states can give rise to similar measured values; [2] the observed intensity depends on the details of the experimental setup in ways that are difficult to calibrate, making quantitative measurements highly challenging.

Additional metabolic information can be extracted by using FLIM to measure the distribution of times NADH and FAD spend in their excited states (54, 55), which strongly depends on the microenvironment of the fluorophores: most importantly, engagement with enzymes leads to a drastic shift in the time NADH and FAD spend in their excited state (35, 56). Thus, FLIM enables measurements reflecting the concentration of NADH and FAD (from intensity) and the extent to which those molecules are engaged with enzymes (from the time they spend in the excited state). There are a variety of different methods for performing FLIM measurements (54). Of these, time-correlated single photon counting (TCSPC) has a number of advantages in terms of photon economy, signal-to-noise, and error analysis, making it well suited for robust, quantitative measurements (57). TCSPC-FLIM uses a laser that generates a high frequency of very short pulses for excitation (Fig. 2C). The power of the laser is kept low enough such that only about one in 100 laser pulses results in the fluorescence molecule producing a photon that can be detected. A sensitive detector enables these individual photons to be counted, and, for each photon, fast electronics allow the precise arrival time of the photon to be determined (Fig. 2D). The arrival times are combined to form a histogram, which represents how long the fluorophores remain in the excited state (Fig. 2E).

Simple fluorophores, such as fluorescein, exhibit an exponential distribution of times in the excited state. In contrast, the histogram of times in the excited state for NADH and FAD are double exponentials, one corresponding to the population of molecules engaged with enzymes and the other corresponding to the population of molecules not engaged with enzymes. By fitting the histogram of photon arrival times to a double exponential, it is possible to measure the fraction of NADH and FAD molecules engaged with enzymes (Fig. 2E). The value of the characteristic lifetime associated with these two states depends on the detailed local environment of NADH and FAD, and FLIM provides information on that as well. FLIM is a microscopy-based technique, producing histograms of times in the excited state for each pixel in an image. Thus, FLIM of NADH and FAD can provide metabolic information with subcellular resolution, limited only by the signal-to-noise of the measurement. In addition, FLIM measurements are relatively robust and are not prone to the experimental artifacts that plague intensity measurements.

FIGURE 2

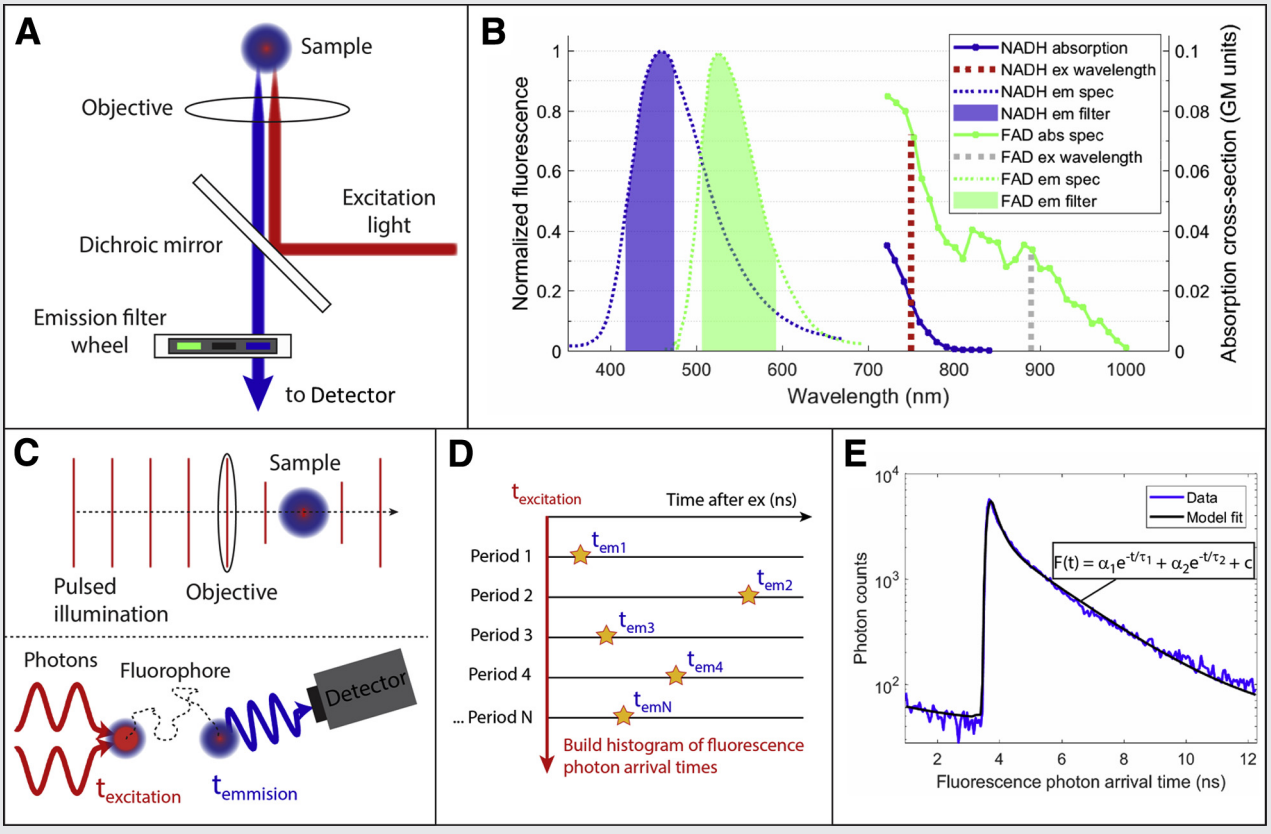

Schematic illustrations of FLIM-based metabolic imaging. (A) Basic components of fluorescence microscopy. Fluorophores are illuminated with excitation light of one wavelength, and fluorescence of a different wavelength is isolated using a combination of a dichroic mirror and emission filter. (B) Two-photon excitation spectra and emission spectra of NADH and FAD. Heikal A. Intracellular coenzymes as natural biomarkers for metabolic activities and mitochondrial anomalies. Biomark Med [Internet] 2010;4:241-263. Fluorescence of each molecule can be isolated using appropriate combinations of excitation wavelengths and emission filters. (C) TCSPC FLIM requires pulsed illumination, where each pulse may excite a single fluorophore. Soon after (picoseconds to nanoseconds), the molecule's emitted fluorescence photon is detected by a single photon counting detector, and fast electronics register its precise arrival time. (D) FLIM delivers pulses at 80 MHz, quickly exciting many fluorophores and recording arrival times. These arrival times are collected into arrival time histograms (at each point in space). (E) Histograms reflect the microenvironment of the fluorophores, and information can be extracted by fitting the fluorescence decays with models, such as the displayed biexponential decay function, which represents the decays of engaged and unengaged molecules. A is a normalization factor, B represents experimental background, τ_1 is the short lifetime, τ_2 is the long lifetime, and *F* is the fraction of molecule engaged with enzymes.

Sanchez. FLIM for egg and embryo assessment. Fertil Steril 2018.

APPLICATION OF FLIM TO THE ASSESSMENT OF OOCYTE AND EMBRYO

Since the metabolism of embryos and oocytes is central to their viability, and since FLIM provides a means of noninvasively and quantitatively measuring metabolism, FLIM is a promising technique for assessing oocyte and embryo viability. We have recently carried out a number of studies on mouse oocytes and embryos to evaluate the safety and potential utility of FLIM within this context (40).

FLIM of NADH and FAD of embryos and oocytes allows their structure to be visualized (Fig. 3A). As NADH is highly concentrated in the mitochondria (58), and FAD is almost entirely localized within the mitochondria (59), both intensity images reflect the distribution of mitochondria. Since aberrations in mitochondrial localization have been associated with mitochondrial dysfunction (60), these images alone may be useful for screening metabolically challenged oocytes and embryos. High-resolution images from FLIM of NADH and FAD can be automatically segmented using image processing (61) and feature recognition algorithms (62), allowing mitochondrial and cytoplasmic regions to be separately integrated (Fig. 3B).

Combining photon arrival times from all pixels in each region into a single histogram leads to high signal-to-noise measurements, which can be fit by a double exponential model (Fig. 3C). Each of these fits provides four metabolic parameters: fraction engaged (*F*), short lifetime (τ_1), long lifetime (τ_2), and average intensity (*I*). With four parameters each from mitochondrial NADH, cytosolic NADH, and mitochondrial FAD (there is no appreciable cytosolic FAD), a single metabolic acquisition yields up to 12 parameters for measuring embryo or oocyte metabolic state (Fig. 3D shows eight metabolic parameters extracted from the NADH measurement). These parameters are highly sensitive to differences and deficiencies in the metabolic state of oocytes and embryos.

FIGURE 3

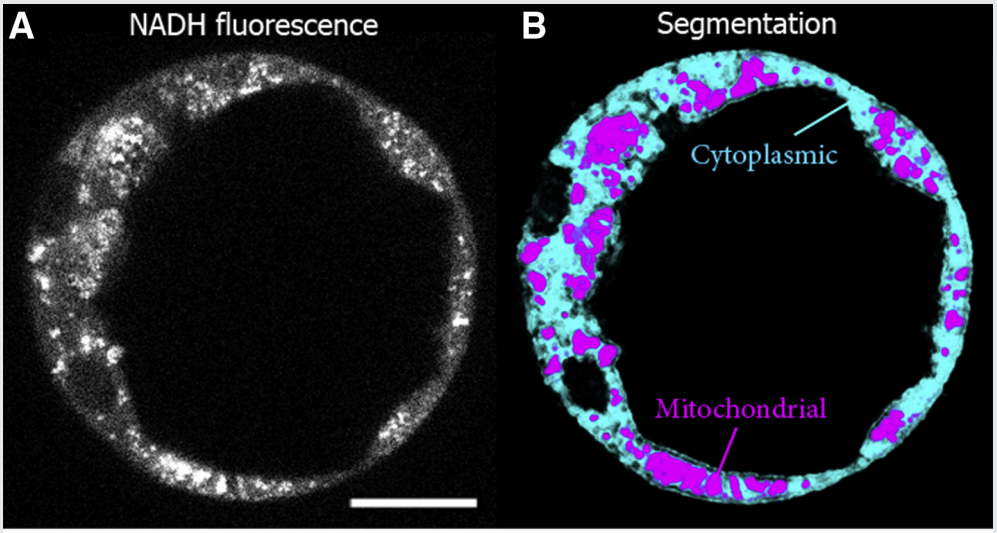

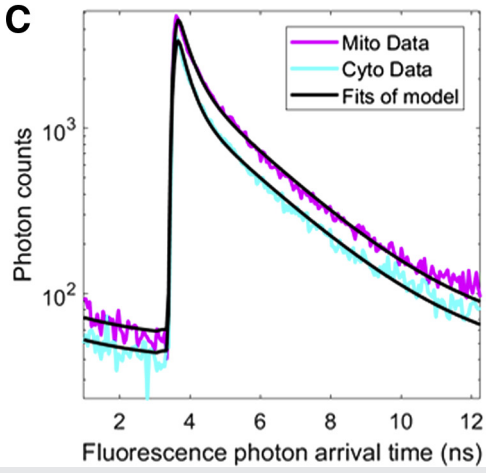

D Quantitative Metabolic Parameters

Mitochondrial	
I: Fluor intensity (au)	7.33±0.04
F: Fraction Bound	0.34±0.03
τ_1: Short lifetime (ns)	0.36±0.04
τ_2: Long lifetime (ns)	2.2±0.2
Cytoplasmic	
I: Fluor intensity (au)	2.851±0.014
F: Fraction Bound	0.29±0.03
τ_1: Short lifetime (ns)	0.31±0.03
τ_2: Long lifetime (ns)	2.2±0.2

FLIM provides quantitative, multiparametric measures of embryo metabolic state. (A) An NADH FLIM intensity image reflects the mitochondrial spatial distribution of a mouse blastocyst, as NADH is highly concentrated in the mitochondria. Scale bar = 25 μm. (B) Image processing and machine learning allow for automated recognition of mitochondrial and cytoplasmic regions. (C) For each of these two segments, all photon arrival times can be binned into a single histogram and fit to a biexponential decay. (D) Fits return quantitative fit parameters, reflecting embryo metabolic state.

Sanchez. FLIM for egg and embryo assessment. Fertil Steril 2018.

In a recent proof-of-concept study, mouse oocytes with significant metabolic dysfunction due to a mutation in a mitochondrial stress response gene exhibited highly significantly different FLIM parameter values compared with wild-type (normal) oocytes (40). Within the same experimental system, mtDNA copy number was only marginally different between the groups. FLIM was also used to compare oocytes from old (1-year-old) versus young mice as a model for mild metabolic dysfunction and showed highly significant differences; mtDNA copy number was not significantly different between the groups (40). Furthermore, FLIM metabolic parameters change over the course of preimplantation embryo development, as the embryo's metabolism reconfigures. Parameters also undergo a large shift in response to mitochondria poisons and changing culture media and oxygen tension (unpublished). Taken together, these results show that FLIM of NADH and FAD can detect biologically relevant differences in the metabolism of oocytes and embryos.

Metabolic imaging with FLIM serves as a powerful research tool for elucidating fundamental aspects of embryo and oocyte metabolism. Studies aimed at determining how oocytes and preimplantation embryos respond to environmental cues such as changes in nutrient and gas content in the culture environment would largely benefit from this sensitive assay. We can also be cautiously optimistic for a potential application in clinical IVF, despite the failure of previous attempts at exploiting metabolic and metabolomics parameters as an embryo viability test. One advantage of FLIM is that the metabolic assessment is done directly in the cell,

without being affected by the dilution and variation associated with spent culture media analyses. Nevertheless, clinical application will require a number of challenging steps, including development of sophisticated algorithms for viability prediction, nonselection studies to determine the diagnostic accuracy of the technique, and randomized clinical trials to demonstrate benefit.

CONCLUSIONS

Metabolism is a key determinant of cell survival, and metabolic parameters could be exploited to improve our understanding of oocyte and embryo viability. Within this context, metabolic imaging via FLIM offers new and potentially useful diagnostic potential by detecting natural fluorescence of FAD and NADH, the two electron transporters that play a central role in OXPHOS. FLIM has been used for metabolic imaging of a variety of systems and most recently has been shown to effectively assess oocyte metabolic state in mouse models of severe and mild metabolic dysfunction. It is likely that FLIM technology will be very useful for experimental studies aimed at improving our understanding of oocyte and embryo metabolism. In addition, FLIM could potentially be implemented as a noninvasive embryo viability test in assisted reproduction, pending appropriate studies.

REFERENCES

1. Steptoe PC, Edwards RG. Birth after the reimplantation of a human embryo. Lancet 1978;2:366.
2. Speirs AL, Lopata A, Gronow MJ, Kellow GN, Johnston WI. Analysis of the benefits and risks of multiple embryo transfer. Fertil Steril 1983;39:468–71.
3. O'Neill C, Saunders DM. Assessment of embryo quality. Lancet 1984;324:1035.
4. Edwards RG, Fishel SB, Cohen J, Fehilly CB, Purdy JM, Slater JM, et al. Factors influencing the success of in vitro fertilization for alleviating human infertility. J In Vitr Fertil Embryo Transf 1984;1:3–23.
5. Veeck LL. An atlas of human gametes and conceptuses: an illustrated reference for assisted reproduction technology. New York: Parthenon Publishing; 1999.
6. Gerris J, De Neubourg D, Mangelschots K, Van Royen E, Van De Meerssche M, Valkenburg M. Prevention of twin pregnancy after in-vitro fertilization or intracytoplasmic sperm injection based on strict embryo criteria: a prospective randomized clinical trial. Hum Reprod 1999;14:2581–7.
7. Van Royen E, Mangelschots K, De Neubourg D, Valkenburg M, Van De Meerssche MV, Ryckaert G, et al. Characterization of a top quality embryo, a step towards single-embryo transfer. Hum Reprod 1999;14:2345–9.
8. Gardner D, Schoolcraft W. In vitro culture of human blastocyst. In: Towards reproductive certainty: infertility and genetics beyond. Carnforth: Parthenon Press; 1999:378–88.
9. Gardner DK, Sakkas D. Human gametes and preimplantation embryos. New York: Springer New York; 2013.
10. Armstrong S, Vail A, Mastenbroek S, Jordan V, Farquhar C. Time-lapse in the IVF-lab: how should we assess potential benefit? Hum Reprod 2015;30:3–8.
11. Armstrong S, Arroll N, Cree LM, Jordan V, Farquhar C. Time-lapse systems for embryo incubation and assessment in assisted reproduction. Cochrane Database Syst Rev 2015;2:CD011320.
12. Adashi EY, Barri PN, Berkowitz R, Braude P, Bryan E, Carr J, et al. Infertility therapy-associated multiple pregnancies (births): an ongoing epidemic. Reprod Biomed Online 2003;7:515–42.
13. Gardner DK, Wale PL. Analysis of metabolism to select viable human embryos for transfer. Fertil Steril 2013;99:1062–72.
14. Practice Committees of SART and ASRM. Elective single-embryo transfer. Fertil Steril 2012;97:835–42.
15. Fragouli E, Alfarawati S, Spath K, Jaroudi S, Sarasa J, Enciso M, et al. The origin and impact of embryonic aneuploidy. Hum Genet 2013;132:1001–13.
16. Hassold T, Abruzzo M, Adkins K, Griffin D, Merrill M, Millie E, et al. Human aneuploidy: incidence, origin, and etiology. Environ Mol Mutagen 1996;175:167–75.
17. Sugiura-Ogasawara M, Ozaki Y, Katano K, Suzumori N, Kitaori T, Mizutani E. Abnormal embryonic karyotype is the most frequent cause of recurrent miscarriage. Hum Reprod 2012;27:2297–303.
18. Scott RT, Upham KM, Forman EJ, Hong KH, Scott KL, Taylor D, et al. Blastocyst biopsy with comprehensive chromosome screening and fresh embryo transfer significantly increases in vitro fertilization implantation and delivery rates: a randomized controlled trial. Fertil Steril 2013;100:697–703.
19. Forman EJ, Hong KH, Ferry KM, Tao X, Taylor D, Levy B, et al. In vitro fertilization with single euploid blastocyst transfer: a randomized controlled trial. Fertil Steril 2013;100:100–7.e1.
20. Munne S, Kaplan B, Frattarelli JL, Gysler M, Child TJ, Nakhuda G, et al. Global multicenter randomized controlled trial comparing single embryo transfer with embryo selected by preimplantation genetic screening using next-generation sequencing versus morphologic assessment. Fertil Steril 2017;108(3 Suppl):e19.
21. Harper J, Jackson E, Sermon K, Aitken RJ, Harbottle S, Mocanu E, et al. Adjuncts in the IVF laboratory: where is the evidence for "add-on" interventions? Hum Reprod 2017;32:485–91.
22. Capalbo A, Ubaldi FM, Rienzi L, Scott R, Treff N. Detecting mosaicism in trophectodermbiopsies: current challenges and future possibilities. Hum Reprod 2017;32:492–8.
23. Vega M, Jindal S. Mosaicism: throwing the baby out with the bath water? J Assist Reprod Genet 2017;34:11–3.
24. Fragouli E, Spath K, Alfarawati S, Kaper F, Craig A, Michel CE, et al. Altered levels of mitochondrial DNA are associated with female age, aneuploidy, and provide an independent measure of embryonic implantation potential. Obstet Gynecol Surv 2016;71:28–9.
25. Victor AR, Brake AJ, Tyndall JC, Griffin DK, Zouves CG, Barnes FL, et al. Accurate quantitation of mitochondrial DNA reveals uniform levels in human blastocysts irrespective of ploidy, age, or implantation potential. Fertil Steril 2017;107:34–42.e3.
26. Sanchez T, Seidler EA, Gardner DK, Needleman D, Sakkas D. Will noninvasive methods surpass invasive for assessing gametes and embryos? Fertil Steril 2017;108:730–7.
27. Leese HJ, Hooper MAK, Edwards RG, Ashwood-Smith MJ. Uptake of pyruvate by early human embryos determined by a non-invasive technique. Hum Reprod 1986;1:181–2.
28. Gardner DK, Leese HJ. Assessment of embryo viability prior to transfer by the noninvasive measurement of glucose uptake. J Exp Zool 1987;242:103–5.
29. Brison DR, Houghton FD, Falconer D, Roberts SA, Hawkhead J, Humpherson PG, et al. Identification of viable embryos in IVF by non-invasive measurement of amino acid turnover. Hum Reprod 2004;19:2319–24.
30. Seli E, Sakkas D, Scott R, Kwok SC, Rosendahl SM, Burns DH. Noninvasive metabolomic profiling of embryo culture media using Raman and near-infrared spectroscopy correlates with reproductive potential of embryos in women undergoing in vitro fertilization. Fertil Steril 2007;88:1350–7.
31. Scott R, Seli E, Miller K, Sakkas D, Scott K, Burns DH. Noninvasive metabolomic profiling of human embryo culture media using Raman spectroscopy predicts embryonic reproductive potential: a prospective blinded pilot study. Fertil Steril 2008;90:77–83.
32. Hardarson T, Ahlstrm A, Rogberg L, Botros L, Hillensj T, Westlander G, et al. Non-invasive metabolomic profiling of day 2 and 5 embryo culture medium: a prospective randomized trial. Hum Reprod 2012;27:89–96.
33. Vergouw CG, Kieslinger DC, Kostelijk EH, Botros LL, Schats R, Hompes PG, et al. Day 3 embryo selection by metabolomic profiling of culture medium with near-infrared spectroscopy as an adjunct to morphology: a randomized controlled trial. Hum Reprod 2012;27:2304–11.
34. Lakowicz JR. Principles of fluorescence spectroscopy. 3d ed. Springer; 2006.
35. Ghukasyan VV, Heikal AA. Natural biomarkers for cellular metabolism: biology, techniques, and applications. CRC Press; 2014.

36. Yu Q, Heikal AA. Two-photon autofluorescence dynamics imaging reveals sensitivity of intracellular NADH concentration and conformation to cell physiology at the single-cell level. J Photochem Photobiol B 2009;95:46–57.
37. Niesner R, Peker B, Schlüsche P, Gericke K-H. Noniterative biexponential fluorescence lifetime imaging in the investigation of cellular metabolism by means of NAD(P)H autofluorescence. Chemphyschem 2004;5:1141–9.
38. Vishwasrao HD, Heikal A, Kasischke K, Webb WW. Conformational dependence of intracellular NADH on metabolic state revealed by associated fluorescence anisotropy. J Biol Chem 2005;280:25119–26.
39. Stringari C, Cinquin A, Cinquin O, Digman MA, Donovan PJ, Gratton E. Phasor approach to fluorescence lifetime microscopy distinguishes different metabolic states of germ cells in a live tissue. Proc Natl Acad Sci U S A 2011;108:13582–7.
40. Sanchez T, Wang T, Pedro MV, Zhang M, Esencan E, Sakkas D, et al. Metabolic imaging with the use of fluorescence lifetime imaging microscopy (FLIM) accurately detects mitochondrial dysfunction in mouse oocytes. Fertil Steril 2018;110:1387–97.
41. Gispert S, Parganlija D, Klinkenberg M, Dröse S, Wittig I, Mittelbronn M, et al. Loss of mitochondrial peptidase clpp leads to infertility, hearing loss plus growth retardation via accumulation of CLPX, mtDNA and inflammatory factors. Hum Mol Genet 2013;22:4871–87.
42. Wang T, Babayev E, Jiang Z, Li G, Zhang M, Esencan E, et al. Mitochondrial unfolded protein response gene Clpp is required to maintain ovarian follicular reserve during aging, for oocyte competence, and development of preimplantation embryos. Aging Cell 2018;17:1–13.
43. Akram M. Citric acid cycle and role of its intermediates in metabolism. Cell Biochem Biophys 2014;68:475–8.
44. Alberts B, Johnson A, Lewis J, Morgan D, Raff M, Roberts K, et al. Molecular biology of the cell. 6th ed. New York: Garland Science; 2014.
45. Barile M, Passarella S, Danese G, Quagliariello E. Rat liver mitochondria can synthesize nicotinamide adenine dinucleotide from nicotinamide mononucleotide and ATP via a putative matrix nicotinamide mononucleotide adenylyltransferase. Biochem Mol Biol Int 1996;38:297–306.
46. Pittelli M, Formentini L, Faraco G, Lapucci A, Rapizzi E, Cialdai F, et al. Inhibition of nicotinamide phosphoribosyltransferase: cellular bioenergetics reveals a mitochondrial insensitive NAD pool. J Biol Chem 2010;285:34106–14.
47. Ying W, Alano CC, Garnier P, Swanson RA. NAD+ as a metabolic link between DNA damage and cell death. J Neurosci Res 2005;79:216–23.
48. Alano CC, Garnier P, Ying W, Higashi Y, Kauppinen TM, Swanson RA. NAD+ depletion is necessary and sufficient for poly(ADP-ribose) polymerase-1-mediated neuronal death. J Neurosci 2010;30:2967–78.
49. Zipfel WR, Williams RM, Christie R, Nikitin AY, Hyman BT, Webb WW. Live tissue intrinsic emission microscopy using multiphoton-excited native fluorescence and second harmonic generation. Proc Natl Acad Sci U S A 2003;100:7075–80.
50. Chance B, Schoener B, Oshino R. Oxidation-reduction ratio studies of mitochondria in freeze-trapped samples. NADH and flavoprotein fluorescence signals. J Biol Chem 1979;254:4764–71.
51. Heikal A. Intracellular coenzymes as natural biomarkers for metabolic activities and mitochondrial anomalies. Biomark Med 2010;4:241–63.
52. Walsh AJ, Cook RS, Manning HC, Hicks DJ, Lafontant A, Arteaga CL, et al. Optical metabolic imaging identifies glycolytic levels, subtypes, and early-treatment response in breast cancer. Cancer Res 2013;73:6164–74.
53. Quinn KP, Sridharan GV, Hayden RS, Kaplan DL, Lee K, Georgakoudi I. Quantitative metabolic imaging using endogenous fluorescence to detect stem cell differentiation. Sci Rep 2013;3:3432.
54. Becker W. Fluorescence lifetime imaging—techniques and applications. J Microsc 2012;247:119–36.
55. Heikal AA. A multiparametric imaging of cellular coenzymes for monitoring metabolic and mitochondrial activities, Reviews in Fluorescence, vol 2010. In: Geddes C, editor. Reviews in fluorescence 2010. New York: Springer; 2012.
56. Blinova K, Levine RL, Boja ES, Griffiths GL, Shi ZD, Ruddy B, et al. Mitochondrial NADH fluorescence is enhanced by complex I binding. Biochemistry 2008;47:9636–45.
57. Becker W. The bh TCSPC handbook. 7th ed. Berlin, Germany: Becker & Hickl Gmbh; 2017.
58. Stein LR, Imai SI. The dynamic regulation of NAD metabolism in mitochondria. Trends Endocrinol Metab 2012;23:420–8.
59. Dumollard R, Marangos P, Fitzharris G, Swann K, Duchen M, Carroll J. Sperm-triggered [Ca2+] oscillations and Ca2+ homeostasis in the mouse egg have an absolute requirement for mitochondrial ATP production. Development 2004;131:3057–67.
60. Nagai S, Mabuchi T, Hirata S, Shoda T, Kasai T, Yokota S, et al. Correlation of abnormal mitochondrial distribution in mouse oocytes with reduced developmental competence. Tohoku J Exp Med 2006;210:137–44.
61. Gonzalez RC. Digital image processing. 4th ed. Pearson; 2018.
62. Breiman L. Random forests. Mach Learn 2001;45:1–32.